



HAL
open science

Brillouin scattering in aluminosilicate glasses and melts up to 2550 K. Temperature and composition effects

Pascal Richet, Alain Polian, Dung Vo-Thanh, Yan Bottinga

► **To cite this version:**

Pascal Richet, Alain Polian, Dung Vo-Thanh, Yan Bottinga. Brillouin scattering in aluminosilicate glasses and melts up to 2550 K. Temperature and composition effects. *Journal of Non-Crystalline Solids: X*, 2022, 14, 10.1016/j.nocx.2022.100086 . insu-03643015

HAL Id: insu-03643015

<https://insu.hal.science/insu-03643015>

Submitted on 4 Jun 2022

HAL is a multi-disciplinary open access archive for the deposit and dissemination of scientific research documents, whether they are published or not. The documents may come from teaching and research institutions in France or abroad, or from public or private research centers.

L'archive ouverte pluridisciplinaire **HAL**, est destinée au dépôt et à la diffusion de documents scientifiques de niveau recherche, publiés ou non, émanant des établissements d'enseignement et de recherche français ou étrangers, des laboratoires publics ou privés.



Distributed under a Creative Commons Attribution 4.0 International License



Brillouin scattering in aluminosilicate glasses and melts up to 2550 K. Temperature and composition effects

Pascal Richet^a, Alain Polian^{b,*}, Dung Vo-Thanh^a, Yan Bottinga^{a,1}

^a Institut de Physique du Globe de Paris, 1 rue Jussieu, 75005 Paris, France

^b IMPMC, CNRS and Sorbonne Université UMR 7590, B 115, 4 place Jussieu, 75005 Paris, France

ARTICLE INFO

Keywords:

Brillouin scattering
Aluminosilicate glass
High temperature

ABSTRACT

Hypersonic sound velocities have been measured by Brillouin scattering for glasses and liquids of the system CaO-MgO-Al₂O₃-SiO₂ (CMAS). Transverse wave velocities are reported for ten samples from 293 up to temperatures ranging from 1000 to 1600 K, depending on composition, and longitudinal velocities for six samples from 293 to the interval 1890–2360 K. For the 13 CMAS compositions, the temperature dependences of acoustic velocities are constant within three temperature intervals: (i) from 293 K to the standard glass transition temperature T_g , (ii) from T_g to the temperature T_{rx} of the onset of structural relaxation at the timescale of Brillouin scattering where transverse waves disappear, (iii) and finally above T_{rx} where only longitudinal waves thus remain observed. The implications of these results for structural relaxation, shear-wave propagation and shear modulus are then discussed.

1. Introduction

The dynamics of particles in a material causes density fluctuations and local variations of the dielectric constant. As a result, part of a beam of light passing through the substance is scattered. Owing to the phase velocity of the acoustic wave, the frequency of the scattered light is Doppler shifted with respect to that of the incident light. The effect is known as Brillouin scattering. Its observation allows one to determine the velocities of both longitudinal (or compressional, V_L) and transverse (or shear, V_T) waves of a material and of its elastic constants too.

For molten silicates, the experimental difficulties opposing Brillouin experiments at the relevant high temperatures were solved in the 1990s, which made measurements of both V_L and V_T possible up to about 1400 K [1–3]. Two distinct temperature intervals were distinguished in which the observed temperature-sound velocity relationships are linear for both velocities. They are separated by clear slope changes at the standard glass transition temperature T_g . Hence, an interesting feature is that V_T can still be measured above T_g although the sample has macroscopically become a liquid. The reason is that Brillouin scattering probes only the solid-like response of the material during light-phonon interactions because configurational changes are much too slow to take place at the 10^{-10} – 10^{-11} s. timescale of the experiments. Since sound velocities

decrease when the density of a material decreases, the breaks in the temperature-velocity relationships for V_L and V_T thus simply signal the enhancement of thermal expansion that takes place at the glass transition [3].

The timescale of structural relaxation characterizes the rate of the configurational rearrangements through which a substance tends to reach internal thermodynamic equilibrium. They are of the order of 1000 s at the standard glass transition, but may decrease with highly increasing temperatures in silicate melts to the point of becoming as short as the timescale of Brillouin scattering. Relaxation effects then manifest themselves through the disappearance of transverse waves and an important decrease of the longitudinal modulus [4,5] and in a further decrease of V_L down to the equilibrium values yielded by ultrasonic measurements, which are performed at MHz frequencies [6,7].

Even though wave velocities represent sensitive probes of the structure and dynamics of melts, Brillouin experiments above 1400 K have remained scarce and the way in which transverse waves disappear upon further heating has apparently not been documented yet for silicates. For V_L , measurements have been extended to 2340 K [6] and then to 2630 K [7] for some alkaline earth aluminosilicates, and to 2300 K for both V_L and V_T of SiO₂ [8]. To complement and extend these results to a wider composition range (Fig. 1), we report new measurements up the

* Corresponding author.

E-mail address: alain.polian@sorbonne-universite.fr (A. Polian).

¹ Deceased.

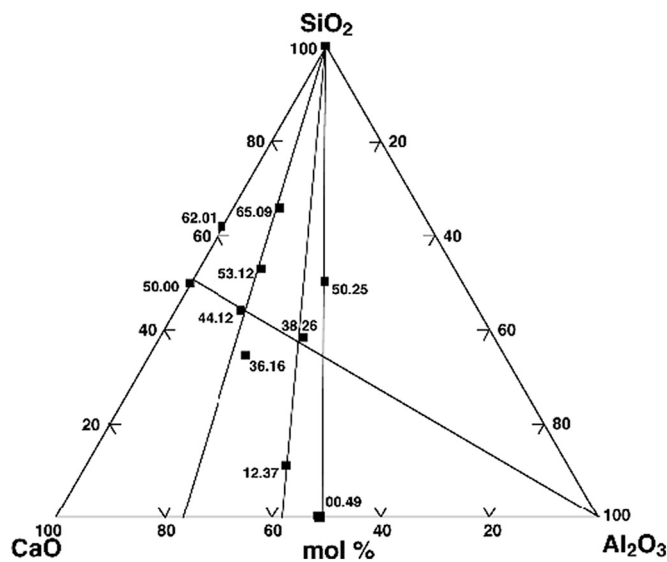


Fig. 1. Compositions investigated in the system CaO-Al₂O₃-SiO₂.

maximum temperatures at which meaningful signals could be recorded. These deal with V_T for ten compositions as well as with V_L in terms of three more samples and additional data for three others. Again, compositions of the system CaO-MgO-Al₂O₃-SiO₂ (CMAS) have been selected in view of their natural and industrial importance, their stability at very high temperatures, and the wide composition range over which they can be studied.

With the new data, a set of consistent V_L and V_T measurements is now available for pure SiO₂ and 10 different CMAS compositions and V_L data only for three additional ones. Referring to a further paper for a detailed analysis of the elastic data in structural terms, we will focus in the present study on the dynamical picture itself as revealed by a much extended temperature range of the Brillouin experiments.

2. Experimental methods and data treatment

Most of the samples belong to the geochemically relevant part of the CMAS system. They were originally prepared for high-temperature density studies [9–12]. Their chemical compositions are listed in Table 1 where labels directly indicate the SiO₂, Al₂O₃, MgO and CaO contents. For example, the Ca65.09 sample is made up of 65 mol% SiO₂, 9 mol% Al₂O₃ and 26 mol% CaO whereas CaMg44.13/21 denotes 44 mol% SiO₂, 13 mol% Al₂O₃, 21 mol% MgO and 22 mol% CaO.

The high-temperature experiments were made with a heating-wire technique up to maximum temperatures of 2000 and 2700 K with Pt₉₀Rh₁₀ and Ir filaments, respectively [13]. Temperatures were determined from the electrical power delivered to the cell as calibrated from the known melting points of a series of compounds. Owing to Ir volatilization, the resulting errors are larger with Ir than with Pt₉₀Rh₁₀ filaments but they remained to within 2% of the reported temperatures. Even though the sample volume was much smaller than 1 mm³, a recurrent problem was incipient sample crystallization above T_g that usually took place after variable extents of supercooling from either the glass transition or the liquidus. Measurements made upon heating or cooling yielded undistinguishable results, as did those obtained in duplicate experiments. From such observations, the combined uncertainties on the reported frequency shifts are estimated to be lower than 1.5 and 3% at the lowest and highest temperatures, respectively. Regarding glass compositions, any initial heterogeneities and changes during the experiments were thus insignificant.

The Brillouin spectra were recorded with a 6-pass Sandercock interferometer [14]. The scattering angle was either 180° or 90° for V_L and 90° for V_T . To perform the measurements with both geometries, the

Table 1

Chemical composition (mol fractions)^a, index of refraction (n) and room-temperature density (ρ) of the samples.

| | SiO ₂ | Al ₂ O ₃ | CaO | MgO | n | ρ (g/cm ³) |
|---------------------------|------------------|--------------------------------|-------|-------|-------|-----------------------------|
| Ca65.09 ^b | 0.648 | 0.088 | 0.264 | | 1.557 | 2.616 |
| Ca62.01 ^c | 0.616 | 0.006 | 0.378 | | 1.582 | 2.756 |
| Ca53.12 ^b | 0.525 | 0.121 | 0.354 | | 1.589 | 2.733 |
| Mg51.01 ^d | 0.512 | 0.005 | 0.003 | 0.481 | 1.580 | 2.745 |
| CaMg51.00/23 ^d | 0.506 | 0.005 | 0.261 | 0.228 | 1.607 | 2.834 |
| Ca50.00 ^d | 0.496 | 0.005 | 0.499 | | 1.610 | 2.895 |
| Ca50.25 ^d | 0.496 | 0.246 | 0.257 | | 1.574 | 2.580 |
| Ca44.12 ^{c,e} | 0.436 | 0.124 | 0.441 | | 1.620 | 2.837 |
| CaMg44.13:21 ^e | 0.438 | 0.125 | 0.225 | 0.212 | 1.621 | 2.740 |
| Ca38.26 ^c | 0.378 | 0.265 | 0.357 | | 1.611 | 2.760 |
| Ca36.16 ^c | 0.363 | 0.155 | 0.482 | | 1.628 | 2.840 |
| Ca12.37 ^{f,g} | 0.116 | 0.371 | 0.513 | | 1.649 | 2.875 |
| Ca00.49 ^e | 0.001 | 0.485 | 0.514 | | 1.643 | 2.918 |

^a Courtial and Dingwell [11,12], except for Ca53.12 [10].

^b Newly investigated composition for both V_L and V_T .

^c Newly investigated composition for only V_T .

^d New V_L and V_T measurements complementing previously published V_L data [6].

^e Samples approximating mineral compositions, namely, Mg51.01: enstatite (CaSiO₃); CaMg51.00/23: diopside ([CaMg]Si₂O₆); Ca50.00: wollastonite (CaSiO₃); Ca50.25: anorthite (CaAl₂Si₂O₈); and Ca44.12: grossular (Ca₃Al₂Si₃O₁₂).

^f Composition for which only V_L data are available [7].

^g Newly investigated composition for only V_L .

samples were loaded in two perpendicular holes drilled by spark erosion in the 1 mm in diameter heating wire [6,7], see Fig. 2. The incident light was the 514.5 nm radiation of an Ar⁺ laser. The frequency of the diffracted light was about 10 GHz. The acoustic velocities were calculated from the equation:

$$V_{L,T} = \Delta\sigma_{L,T} \lambda_i / [2 n \sin(\vartheta/2)], \quad (1)$$

where $\Delta\sigma_{L,T}$ is the measured frequency shift, λ the wave length of the incident light, n the index of refraction of the sample and ϑ the scattering angle, which was either 90 or 180° for the longitudinal waves and 90° for the transverse waves.

The refractive indices are the only unknown parameters in eq. (1). They were approximated as done before [6]. Because their variations with temperature are small the important parameters are the room-temperature values, which are accordingly listed in Table 1. Once sound velocities are known the longitudinal (M_L) and shear (G_s) moduli are evaluated with

$$M_L = \rho V_L^2, \quad (2a)$$

$$G_s = \rho V_T^2, \quad (2b)$$

where ρ is the sample density. Knowing M_L and G_s we finally evaluated the adiabatic bulk modulus, B_s , which is the reciprocal of the adiabatic compressibility, with

$$B_s = M_L - 4 G_s / 3. \quad (3)$$

Our Brillouin setup is not designed to determine the intensity of the central Rayleigh line so we could not determine the relaxed adiabatic bulk moduli of melts from the so-called Placzek-Landau ratio.

Evaluation of eq. (2) requires to know the density as well as its variation with temperature for the 13 compositions of Table 1. The thermal expansion coefficients used are listed in Table 2. The room-temperature densities are known accurately (Table 1) but not the thermal expansion coefficients (α) of the samples from 300 to the high temperatures reached in our study. Because of the large increase in dilation that takes place at the glass transition, these coefficients must be evaluated for both the glass (α_{gl}) and liquid (α_{liq}) phases.

For liquids, available measurements indicate that α can also be considered constant from the liquidus to temperatures as high as 2100 K

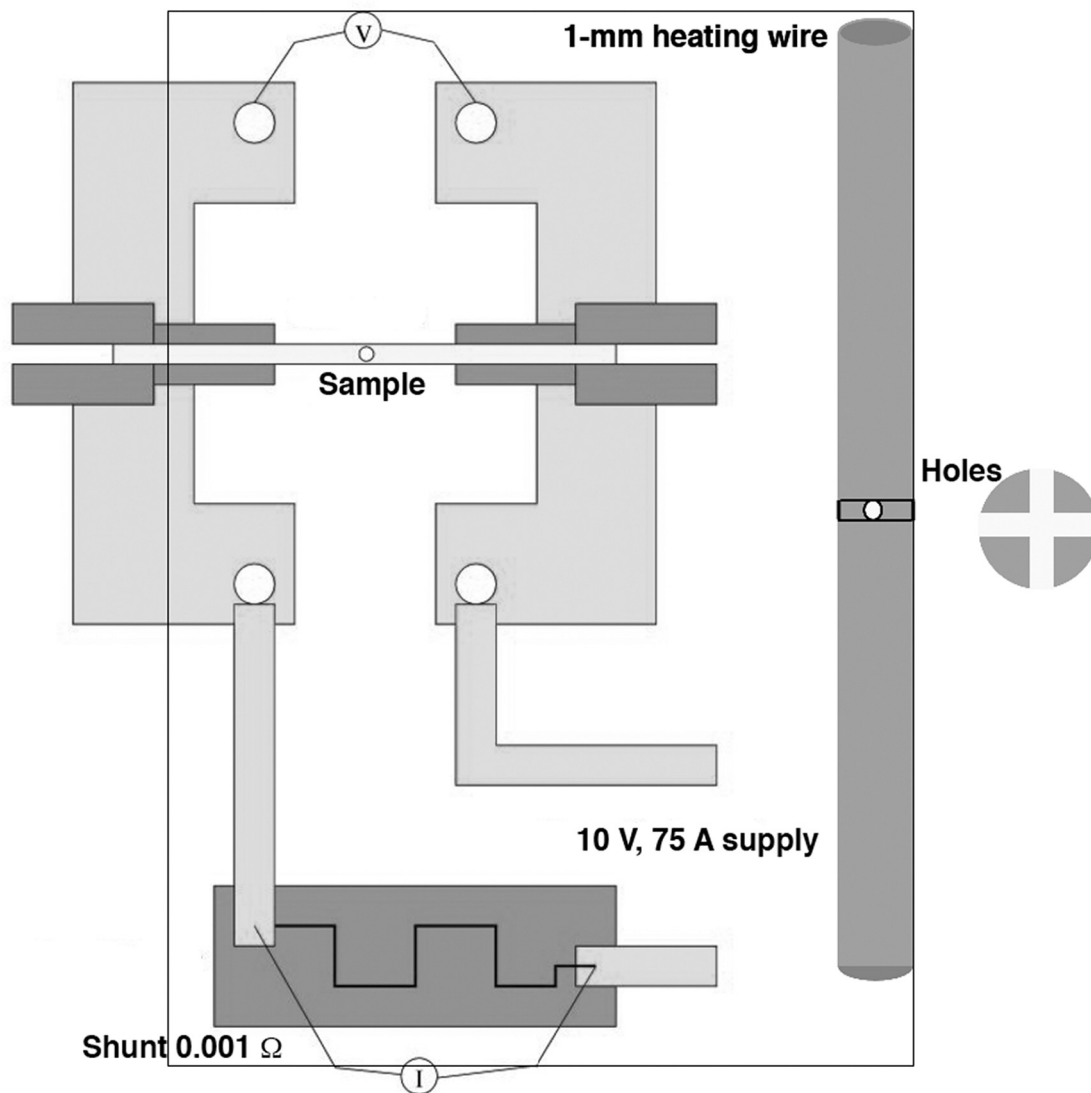


Fig. 2. High-temperature heating-wire setup.

Table 2
Coefficients of thermal expansion (K^{-1}) used in different temperature intervals^a.

| | $293-T_g$ | T_g-T_{rx} | $T > T_{rx}$ |
|--------------|----------------------|----------------------|----------------------|
| Ca65.09 | $1.55 \cdot 10^{-5}$ | $4.40 \cdot 10^{-5}$ | $5.02 \cdot 10^{-5}$ |
| Ca62.01 | $1.91 \cdot 10^{-5}$ | $11.2 \cdot 10^{-5}$ | $6.19 \cdot 10^{-5}$ |
| Ca53.12 | $1.74 \cdot 10^{-5}$ | $5.76 \cdot 10^{-5}$ | $5.63 \cdot 10^{-5}$ |
| Mg51.01 | $1.06 \cdot 10^{-5}$ | $33.0 \cdot 10^{-5}$ | $3.45 \cdot 10^{-5}$ |
| CaMg51.00/23 | $1.80 \cdot 10^{-5}$ | $13.2 \cdot 10^{-5}$ | $5.38 \cdot 10^{-5}$ |
| Ca50.00 | $2.66 \cdot 10^{-5}$ | $9.48 \cdot 10^{-5}$ | $8.63 \cdot 10^{-5}$ |
| Ca50.25 | $1.62 \cdot 10^{-5}$ | $3.49 \cdot 10^{-5}$ | $5.25 \cdot 10^{-5}$ |
| Ca44.12 | $2.84 \cdot 10^{-5}$ | $3.69 \cdot 10^{-5}$ | $9.21 \cdot 10^{-5}$ |
| CaMg44.13/21 | $1.08 \cdot 10^{-5}$ | $7.11 \cdot 10^{-5}$ | $3.51 \cdot 10^{-5}$ |
| Ca38.26 | $1.37 \cdot 10^{-5}$ | $4.24 \cdot 10^{-5}$ | $4.45 \cdot 10^{-5}$ |
| Ca36.16 | $1.82 \cdot 10^{-5}$ | $3.16 \cdot 10^{-5}$ | $5.89 \cdot 10^{-5}$ |
| Ca12.37 | $1.71 \cdot 10^{-5}$ | $3.51 \cdot 10^{-5}$ | $5.54 \cdot 10^{-5}$ |
| Ca00.49 | $0.78 \cdot 10^{-5}$ | $8.05 \cdot 10^{-5}$ | $2.54 \cdot 10^{-5}$ |

^a T_g and T_{rx} as listed in Table 5.

(e.g., [10–12,15]). But the situation is more controversial between T_g and the liquidus. Whereas it was stated that α_{liq} is the same as above the liquidus [16], measurements for CaMg51.00/23 and Ca50.25 liquids have indicated that it decreases with increasing temperatures [17,18]. Because of the scarcity of such measurements, however, this effect could

not be considered for most of our samples. Hence, we assumed constant α_{liq} calculated from the densities reported at T_g and at the high temperature T_{rx} at which the derivative dV_L/dT changes rapidly. This rough way of estimating α_{liq} in this interval for instance results in a value of 13.2×10^{-5} for CaMg51.00/23, whereas values ranging from $10.8 \cdot 10^{-5}$ to $13.9 \cdot 10^{-5}$ have been published [17–19]. For Ca50.25 our estimate of α_{liq} is $3.5 \cdot 10^{-5}$ whereas values of $5.9 \cdot 10^{-5}$ and $5.2 \cdot 10^{-5}$ have been reported [18,19]. As a matter of fact, whether α_{liq} is constant or not is inconsequential for our purpose because of the low sensitivity of the derived sound velocities to the values used for this parameter.

As usually made, we have also assumed that α is constant for the glass phases. For the sake of simplicity, we have used the simple approximation $\alpha_{liq}/\alpha_{gl} = 3.25$. The uncertainties introduced in this way are minor because α_{gl} is very small throughout the CMAS system.

3. Results

The temperature intervals of the reported results varied from a sample to another. For samples that are not good glass formers, crystallization of the supercooled liquid abruptly terminated the experiments while the LA and TA acoustic spectra were still well resolved. In other cases, the wave frequency decreased in such a way that it left the free spectral range of our Fabry-Pérot interferometer. In a third case the

intensity decrease with increasing temperatures was simply such that Brillouin peaks could no longer be identified in the noise background.

As previously observed [6], the Brillouin peaks remain rather narrow from room temperature to the standard glass transition T_g above which they broaden markedly (Figs. 3, 4) because of the progressively increasing number of atomic configurations that become accessible. This is the main reason why the relative precision of the measurements decreases with increasing temperatures. Whenever possible, glass transition temperatures were determined from the breaks on both V_L and V_T although the latter could not be accurate when very small slope changes were observed.

The hypersonic velocities derived from the observed Brillouin frequency shifts and the indices of refraction of Table 1 are reported in Tables 3 and 4 for the longitudinal and transverse measurements, respectively. For the former, only the observations made at 180° have been listed because they are more numerous and tend to show a higher reproducibility than the 90° data with which they nonetheless generally agree to within the stated experimental uncertainties (Fig. 5). Likewise, good agreement is found with previous V_L measurements made up to about 1400 K on some of the same samples [6,7] and on same compositions (i.e., Ca50.25, Ca44.12 and CaMg51.00/23) [3,20]. This applies in particular to the temperatures of the breaks in the slopes of the wave-velocity temperature relationships that delineate intervals in which the

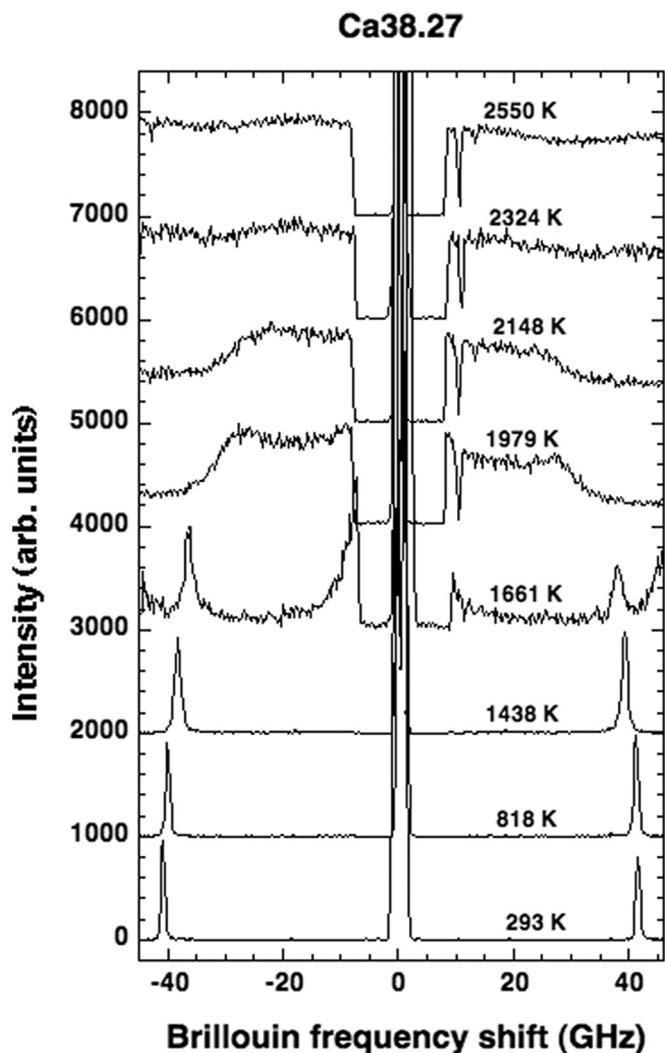


Fig. 3. Changes in the line shapes of the Brillouin longitudinal waves of Ca38.27 from room temperature to 2550 K recorded in the backscattering geometry.

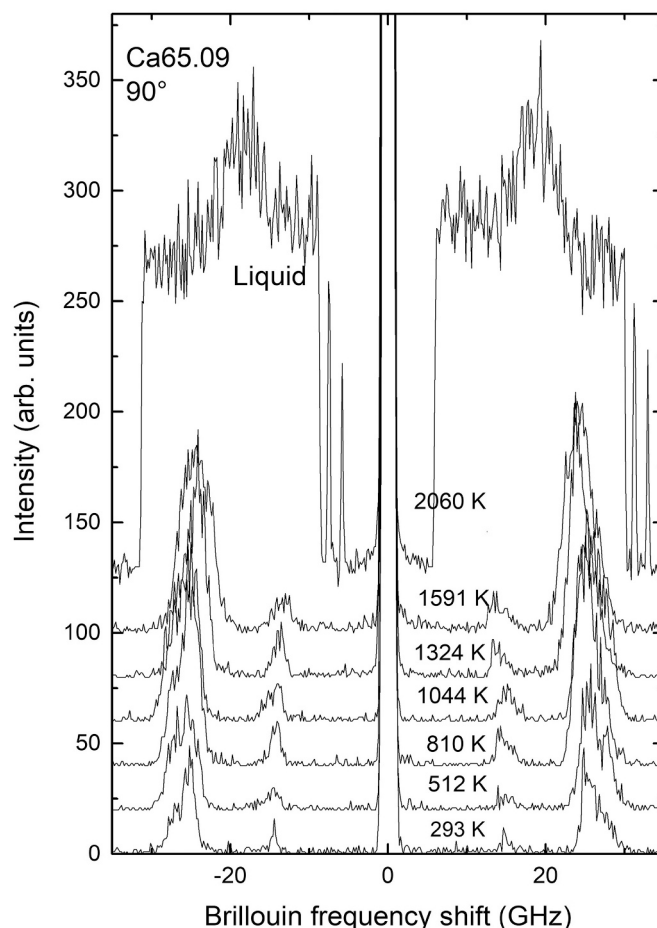


Fig. 4. Brillouin spectra showing longitudinal and transverse modes of Ca65.09 in the 90° geometry at various temperatures. Due to the very high temperature of the heating wire, the stray light increases strongly at 2060 K. The spectra are shifted vertically for clarity.

linear fits are made to the data (Table 5). In contrast to previous results, however, our measurements show the clear breaks previously reported for V_T at the glass transition [3,21] for only part of the samples, namely, Mg51.01, Ca44.12, Ca53.12 and Ca62.01. The reason why they are not seen for Ca65.09, Ca50.25, Ca38.26 and Ca36.16 is unknown. Rather than risking unwarranted explanations drawn from this first series of results at such high temperatures, it is more honest to state that more extensive measurements are required to propose reliable interpretations for such differences.

As expected from the strong attenuation of shear waves in liquids, the maximum temperatures T_{max} at which Brillouin peaks were observed are much lower for the shear than for the longitudinal waves with either the 180° or the 90° geometry. Whereas the latter have been observed up to a record high temperature of 2630 K for Ca36.16 [6], the former were followed up to only 1610 K in the case of Ca38.26. At $T_{max}(V_T)$, the disappearance of the Brillouin peaks for shear waves is sudden with respect to the temperature intervals of about 50°C separating successive measurements. In other words, a slow vanishing of the shear signal was not observed. In contrast, at $T_{max}(V_L)$ the Brillouin peaks for longitudinal hypersonic waves disappeared because they lost their characteristic shapes when becoming drowned in the background noise whose intensity increased continuously with temperature (Figs. 3, 4).

As an example of the wave velocity-temperature relationships, the results for Ca38.26 have been selected because they extend to the nearly record temperature of 2550 K for longitudinal waves [6] and to the aforementioned highest temperature attained for transverse waves

Table 3
Longitudinal sound velocities (m/s).

| Ca65.09 | | Ca53.12 | | Mg51.01 | CaMg51.00/23 | | |
|---------|-------|---------|-------|---------|--------------|------|-------|
| T(K) | V_L | T(K) | V_L | T(K) | V_L | T(K) | V_L |
| 293 | 6196 | 293 | 6411 | 293 | 7163 | 293 | 6521 |
| 293 | 6231 | 293 | 6391 | 346 | 7170 | 293 | 6589 |
| 293 | 6211 | 293 | 6416 | 411 | 7081 | 293 | 6514 |
| 293 | 6216 | 341 | 6431 | 458 | 7108 | 375 | 6523 |
| 350 | 6202 | 416 | 6375 | 515 | 7205 | 465 | 6614 |
| 407 | 6203 | 456 | 6365 | 580 | 7102 | 537 | 6540 |
| 450 | 6218 | 497 | 6384 | 643 | 7069 | 606 | 6548 |
| 494 | 6200 | 542 | 6384 | 730 | 7094 | 669 | 6533 |
| 528 | 6181 | 590 | 6408 | 798 | 7067 | 728 | 6444 |
| 584 | 6186 | 643 | 6321 | 866 | 7076 | 800 | 6506 |
| 643 | 6198 | 702 | 6347 | 948 | 6911 | 880 | 6528 |
| 706 | 6175 | 765 | 6334 | 1012 | 6996 | 925 | 6450 |
| 768 | 6193 | 815 | 6339 | 1061 | 6918 | 989 | 6264 |
| 827 | 6167 | 876 | 6379 | 1118 | 6862 | 1070 | 6147 |
| 890 | 6189 | 926 | 6360 | | | 1105 | 5973 |
| 948 | 6229 | 985 | 6300 | | | 1685 | 4315 |
| 997 | 6249 | 1024 | 6286 | | | 1783 | 4018 |
| 1039 | 6128 | 1068 | 6253 | | | 913 | 6580 |
| 1084 | 6173 | 1113 | 6215 | | | 690 | 6570 |
| 1129 | 6087 | 1158 | 6186 | | | 293 | 6583 |
| 1179 | 6057 | 1191 | 6074 | | | | |
| 1227 | 6011 | 1230 | 6123 | | | | |
| 1277 | 6041 | 1280 | 6052 | | | | |
| 1336 | 5996 | 1317 | 6017 | | | | |
| 1388 | 6006 | 1363 | 6009 | | | | |
| 1444 | 6012 | 1409 | 6015 | | | | |
| 1498 | 5991 | 1450 | 5936 | | | | |
| 1551 | 5972 | 1667 | 5182 | | | | |
| 1614 | 5932 | 1800 | 4646 | | | | |
| 1700 | 5832 | 1895 | 4616 | | | | |
| 1930 | 5254 | 1919 | 4568 | | | | |
| 2033 | 5115 | 1990 | 4148 | | | | |
| 2077 | 4995 | | | | | | |
| 2149 | 4910 | | | | | | |
| 2210 | 4752 | | | | | | |
| 2270 | 4550 | | | | | | |
| 2360 | 4341 | | | | | | |

| Ca50.00 | | Ca50.25 | | Ca12.37 | |
|---------|-------|---------|-------|---------|-------|
| T(K) | V_L | T(K) | V_L | T(K) | V_L |
| 293 | 6409 | 293 | 6619 | 293 | 6486 |
| 324 | 6440 | 293 | 6634 | 293 | 6486 |
| 456 | 6320 | 293 | 6629 | 361 | 6465 |
| 813 | 6163 | 429 | 6608 | 421 | 6453 |
| 1850 | 3799 | 543 | 6603 | 481 | 6441 |
| 2247 | 3450 | 780 | 6603 | 548 | 6424 |
| 2128 | 3451 | 989 | 6647 | 618 | 6426 |
| 2087 | 3492 | 1083 | 6640 | 676 | 6404 |
| 1876 | 3725 | 1199 | 6679 | 752 | 6392 |
| 1540 | 4924 | 1303 | 6452 | 821 | 6366 |
| 1033 | 6282 | 1379 | 6476 | 892 | 6353 |
| 716 | 6356 | 1431 | 6462 | 969 | 6313 |
| 293 | 6432 | 1526 | 6412 | 1040 | 6344 |
| | | 1946 | 5262 | 1097 | 6211 |
| | | 1992 | 5191 | 1144 | 6218 |
| | | 2080 | 4778 | 1191 | 6192 |
| | | 2186 | 4559 | 1241 | 6138 |
| | | 2336 | 4403 | 1800 | 4306 |
| | | | | 1895 | 3936 |

(Fig. 6). For V_T , the picture is simple because a single linear fit accounts for all the data from 293 to 1610 K with a slope $dV_T/dT = -0.367$ m/s. For V_L , four temperature ranges must in contrast be distinguished. The first extends from 293 K to a temperature close to that of the standard glass transition T_g (with $dV_L/dT = -0.17$ m/s); the second ($dV_L/dT = -0.45$ m/s) ranges from T_g to the temperature T_{rx} from which structural relaxation begins to take place; the third ($dV_L/dT = -5.123$ m/s) from T_{rx} to T_{eq} , the temperature at which relaxation is complete; and the fourth ($dV_L/dT = -0.77$ m/s) is that of the relaxed liquid state where the

Brillouin velocity join nicely with the MHz ultrasonic observations at lower temperatures.

Although they do not extend to similarly high temperatures, the results for the other compositions generally conform to the same basic pattern for V_L (Fig. 7). Along with Ca38.26, three other compositions clearly achieved complete relaxation as demonstrated by V_L values lower than the ultrasonic data: (i) 3237 m/s at 2086 K [7] vs. 3324 m/s at 2200 K [22] for Ca00.49; (ii) 2969 m/s at 2300 K [6] vs. 3125 m/s at 2200 K [22] for Ca44.12; and (iii) 3141 m/s at 2281 K vs. nearly the same values [22,23] for Ca50.00. Low V_L values have also been observed for the two mixed (Ca,Mg) melts, but ultrasonic data are then lacking for comparison. For Ca53.12, the lowest value of 4148 m/s measured at 1990 K for (Table 3) is in contrast 1170 m/s higher than the ultrasonic value reported at 1623 K [10]. Even for Ca36.16 at 2630 K the value of 3348 m/s is still 10% too high with respect to the ultrasonic range 2978–2952 m/s of V_L between 1623 and 1823 K [10]. As for Ca50.25, it is the sample that remained the farthest from equilibrium since its lowest V_L of 4403 m/s at 2335 K is still 55% higher than the ultrasonic value at 1833 K [22].

For transverse waves, the picture is more diverse (Fig. 8). An important point, however, is that existing breaks in the V_T - T relationships are found at the same temperatures as for the V_L - T relationships although the magnitude of these changes is not necessarily the same for both kinds of waves. The lack of break at T_g observed for Ca38.26 (Fig. 6) is in fact shared only by Ca65.09, Ca50.25 and Ca36.16 whether their dV_T/dT is zero or negative. Data are lacking above T_g for Ca62.01, Mg51.01 and Ca50.00, but the V_T decrease is clearly enhanced from T_g for Ca53.12 and CaMg51.00/23 and does likely so for Ca62.01 and Ca44.12.

In spite of marked differences of temperature dependences for example exhibited by SiO₂ [8] and Ca00.49, the velocities of transverse and longitudinal waves depend on sample composition in a similar way. This is shown by minor variations of the ratio V_T/V_L , which varies from 0.54 to 0.57 at 293 K, and from 0.49 to 0.57 at T_g . As a matter of fact, pure SiO₂ exhibits a marked rise of both V_L and V_T with increasing temperatures. Especially for transverse waves, the sound velocity difference between pure SiO₂ and aluminosilicates is impressive (Fig. 5). Already at room temperature, V_T is much greater for SiO₂ than for the other compositions, except Mg51.01, which contrasts with the values of V_L that become larger for SiO₂ than for the aluminosilicates only above 1300 K. Since sound velocities generally decrease with increasing temperature and lower densities, pure SiO₂ is one of the best-known counter example whose anomalous properties have been related to a very low, if not negative, thermal expansion caused by decreases of first Si–Si distances [8].

4. Discussion

4.1. Structural relaxation

In previous studies a single temperature regime was identified for V_L above T_g . Of course, the third T_{rx} - T_{eq} interval required experiments above about 1800 K to be satisfactorily defined, but such measurements have also been most useful to give a broader overview and to help detect the less sharp breaks at T_{rx} . Interestingly, the very same interval T_g - T_{rx} is seen in variations of the Full Width at Half Maximum (FWHM) of the Brillouin peak as illustrated in Fig. 9 for Ca65.09. Not only are the temperatures T_g and T_{rx} identical in V_L and FWHM plots, but there is also a close correspondence between the variations of both parameters in the three temperature intervals identified.

Once the additional break at T_r had been clearly revealed by samples such as Ca65.09, Ca53.12, Ca38.26 or Ca36.16, the intermediate intervals T_g - T_{rx} could be identified for other supercooled liquids, albeit with a lower precision when the data are more noisy as found for Ca50.25 (Fig. 6). For this purpose, the fact that the lower bounds of these intervals are close to the standard glass transition temperatures was an

Table 4
Transverse sound velocities (m/s).

| Ca65.09 | | Ca62.01 | | Ca53.12 | | Mg51.01 | | CaMg51.00/23 | |
|---------|-------|---------|-------|---------|-------|---------|-------|--------------|-------|
| T(K) | V_T | T(K) | V_T | T(K) | V_T | T(K) | V_T | T(K) | V_T |
| 293 | 3365 | 293 | 3525 | 293 | 3634 | 293 | 3966 | 293 | 3554 |
| 293 | 3449 | 362 | 3530 | 293 | 3558 | 346 | 3955 | 293 | 3581 |
| 345 | 3438 | 413 | 3479 | 293 | 3620 | 411 | 3883 | 293 | 3506 |
| 400 | 3441 | 471 | 3495 | 345 | 3588 | 458 | 3859 | 373 | 3545 |
| 454 | 3444 | 520 | 3451 | 399 | 3509 | 515 | 3960 | 465 | 3646 |
| 512 | 3447 | 584 | 3476 | 484 | 3549 | 580 | 3916 | 537 | 3589 |
| 575 | 3430 | 637 | 3513 | 539 | 3531 | 643 | 3906 | 606 | 3524 |
| 627 | 3355 | 684 | 3490 | 605 | 3521 | 730 | 3954 | 669 | 3569 |
| 679 | 3394 | 738 | 3506 | 660 | 3635 | 798 | 3868 | 728 | 3496 |
| 723 | 3453 | 786 | 3489 | 719 | 3513 | 866 | 3845 | 800 | 3521 |
| 758 | 3377 | 836 | 3499 | 782 | 3538 | 948 | 3801 | 880 | 3533 |
| 808 | 3366 | 910 | 3517 | 835 | 3527 | 1012 | 3848 | 925 | 3500 |
| 866 | 3347 | 978 | 3480 | 926 | 3456 | 1061 | 3802 | 989 | 3408 |
| 925 | 3287 | 1052 | 3486 | 979 | 3606 | | | 1070 | 3305 |
| 976 | 3311 | 1117 | 3339 | 1040 | 3639 | | | 1105 | 3198 |
| 1040 | 3420 | | | 1090 | 3504 | | | | |
| 1093 | 3359 | | | 1146 | 3495 | | | | |
| 1150 | 3286 | | | 1206 | 3416 | | | | |
| 1200 | 3275 | | | 1258 | 3385 | | | | |
| 1250 | 3263 | | | 1307 | 3297 | | | | |
| 1282 | 3191 | | | 293 | 3654 | | | | |
| 1324 | 3243 | | | | | | | | |
| 1375 | 3303 | | | | | | | | |
| 1420 | 3276 | | | | | | | | |
| 1473 | 3277 | | | | | | | | |
| 1541 | 3154 | | | | | | | | |
| 1591 | 3214 | | | | | | | | |

| Ca50.00 | | Ca50.25 | | Ca44.12 | | Ca38.26 | | Ca36.16 | |
|---------|-------|---------|-------|---------|-------|---------|-------|---------|-------|
| T(K) | V_T |
| 293 | 3599 | 293 | 3523 | 293 | 3512 | 293 | 3732 | 293 | 3794 |
| 293 | 3539 | 293 | 3488 | 500 | 3509 | 377 | 3614 | 293 | 3721 |
| 360 | 3563 | 293 | 3538 | 964 | 3437 | 460 | 3688 | 364 | 3810 |
| 420 | 3587 | 343 | 3568 | 1074 | 3327 | 528 | 3701 | 426 | 3719 |
| 465 | 3562 | 395 | 3573 | 1179 | 3276 | 585 | 3607 | 480 | 3640 |
| 516 | 3633 | 441 | 3633 | 1353 | 3074 | 647 | 3560 | 525 | 3702 |
| 575 | 3541 | 480 | 3626 | 1484 | 2823 | 691 | 3484 | 575 | 3596 |
| 630 | 3544 | 522 | 3580 | 1160 | 3309 | 746 | 3493 | 640 | 3525 |
| 685 | 3523 | 569 | 3632 | 716 | 3387 | 811 | 3481 | 705 | 3568 |
| 733 | 3455 | 612 | 3621 | 293 | 3483 | 881 | 3438 | 766 | 3556 |
| 790 | 3451 | 660 | 3631 | | | 946 | 3506 | 817 | 3429 |
| 866 | 3503 | 710 | 3581 | | | 1010 | 3461 | 866 | 3424 |
| 916 | 3458 | 772 | 3578 | | | 1060 | 3468 | 919 | 3507 |
| 991 | 3476 | 820 | 3533 | | | 1125 | 3435 | 979 | 3381 |
| | | 867 | 3606 | | | 1186 | 3357 | 1046 | 3407 |
| | | 939 | 3561 | | | 1257 | 3404 | 1107 | 3345 |
| | | 977 | 3586 | | | 1306 | 3354 | 1163 | 3369 |
| | | 1008 | 3538 | | | 1356 | 3351 | 1218 | 3232 |
| | | 1058 | 3478 | | | 1402 | 3342 | 1275 | 3230 |
| | | 1096 | 3572 | | | 1448 | 3236 | | |
| | | 1131 | 3462 | | | 1504 | 3309 | | |
| | | 1170 | 3515 | | | 1610 | 3264 | | |
| | | 1194 | 3522 | | | | | | |
| | | 1222 | 3475 | | | | | | |
| | | 1258 | 3464 | | | | | | |
| | | 1299 | 3445 | | | | | | |
| | | 1341 | 3460 | | | | | | |
| | | 1377 | 3421 | | | | | | |
| | | 1423 | 3452 | | | | | | |
| | | 1487 | 3421 | | | | | | |

obvious advantage. For Ca50.00, Mg.50.01 and CaMg51.00/23, however, such determinations were not possible because of a lack of measurements caused by incipient crystallization above T_g (Fig. 7).

These V_L observations are similar to those made at constant frequency in ultrasonic measurements of compressional wave velocities [24] although in this case the transition is shifted to much lower temperatures in view of the 10^5 difference in experimental timescales between the two techniques. At high temperatures, the slight variations of

ultrasonic longitudinal velocities indicate that they refer themselves to structurally relaxed liquids. Hence, a good match to these data [10,22,23] is the simplest criterion for ensuring that structural relaxation has also become complete in Brillouin scattering experiments. For compositions such as Ca36.16, Ca53.12, or Ca62.01, estimating the temperature at which equilibrium values would be obtained could nonetheless be made reliably in view of the narrow extrapolations of the linear $V_L - T$ relationships needed to reach the ultrasonic values.

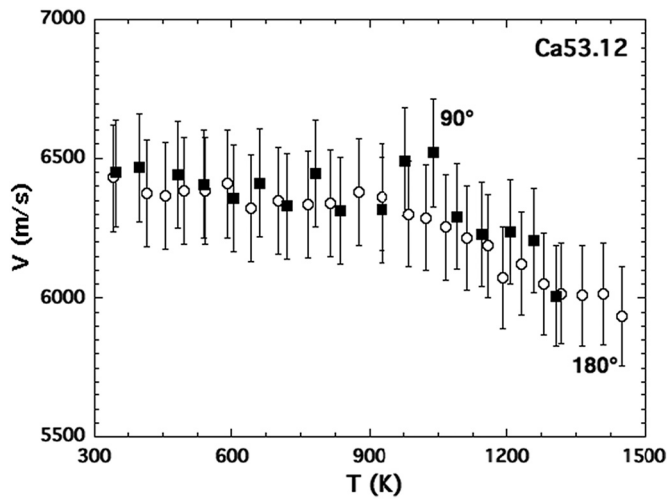


Fig. 5. Comparison of the longitudinal acoustic velocities measured with the 90 (full squares) and 180° (empty circles) geometries for Ca53.12.

Owing to the intrinsic difficulties of experiments made above 2000 K, however, the way in which our Brillouin results join with ultrasonic data might seem imperfect. That agreement is nonetheless within the combined uncertainties of the measurements is shown by analogous observations made on glycerol between 100 and 450 K [25]. Complete relaxation was demonstrated above 400 K by the agreement between compressional wave velocities measured at 15 MHz and 10 GHz, after a similar sequence of events beginning at the glass transition. Together with ultrasonic observations [26], Brillouin measurements for B₂O₃

glass and liquid show the same pattern between 473 and 1500 K [4,5].

4.2. Shear wave propagation and configurational entropy

The maximum temperature above which hypersonic shear waves do not propagate depends on composition (Table 5), but is always lower than T_{rx} , which thus appears to represent an upper bound. Of course, the V_T variations have important consequences for the shear modulus (Fig. 10). Below T_g , the values are frequency independent and vary with

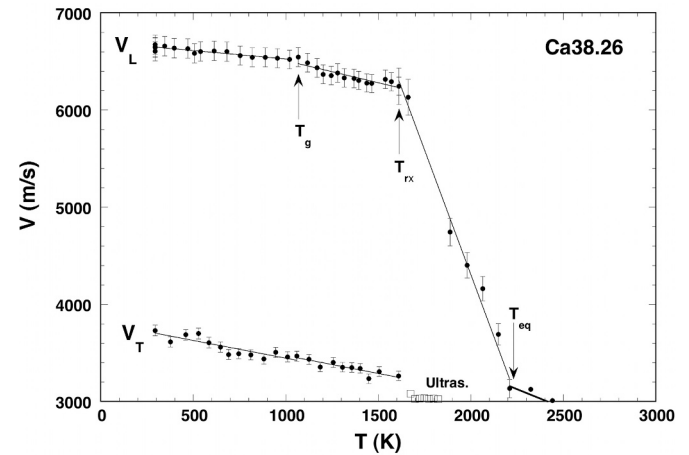


Fig. 6. Hypersonic longitudinal and transverse wave velocities of Ca38.26 glass and liquid in distinct temperature intervals. For comparison, ultrasonic data are included as empty squares [10]. Linear-fit parameters reported in Table 5.

Table 5

Linear fits to the velocity-temperature relationships for longitudinal and transverse hypersonic waves in the different temperature intervals. Data in K and m/s.

| | $V(293)$ | dV/dT | T_g | $V(T_g)$ | dV/dT | T_{rx} | $V(T_{rx})$ | dV/dT | T_{max} | $V(T_{max})$ |
|---------------------|----------|---------|-------|----------|---------|----------|-------------|---------|-----------|--------------|
| Ca65.09 | | | | | | | | | | |
| V_L | 6203 | -0.030 | 1015 | 6185 | -0.460 | 1641 | 5897 | -2.08 | 2350 | 4341 |
| V_T | 3455 | -0.183 | | | | | | | 1591 | 3214 |
| Ca62.01 | | | | | | | | | | |
| V_L | 6208 | -0.024 | 1010 | 6191 | -1.589 | 1273 | 5897 | -2.425 | 2310 | 3275 |
| V_T | 3502 | -0.017 | 1051 | 3439 | | | | | 1117 | 3486 |
| Ca53.12 | | | | | | | | | | |
| V_L | 6408 | -0.130 | 950 | 6323 | -0.760 | 1428 | 5960 | -0.760 | 1990 | 4448 |
| V_T | 3571 | -0.031 | 1068 | 3547 | -0.955 | | | | 1307 | 3297 |
| Mg51.01 | | | | | | | | | | |
| V_L | 7091 | -0.241 | 1065 | 6905 | -3.208 | | | | 2209 | 3421 |
| V_T | 3953 | -0.171 | | | | | | | 1061 | 3802 |
| CaMg51.00/23 | | | | | | | | | | |
| V_L | 6575 | -0.103 | 903 | 6512 | -2.459 | | | | 2340 | 3174 |
| V_T | 3566 | -0.059 | 911 | 3529 | -1.587 | | | | 1105 | 3198 |
| Ca50.00 | | | | | | | | | | |
| V_L | 6413 | -0.306 | 974 | 6205 | -2.423 | | | | 2281 | 3149 |
| V_T | 3592 | -0.191 | | | | | | | 991 | 3476 |
| Ca50.25 | | | | | | | | | | |
| V_L | 6631 | -0.012 | 1072 | 6621 | -0.800 | 1704 | 6116 | -2.840 | 2336 | 4403 |
| V_L | 3605 | -0.120 | | | | | | | 1487 | 3421 |
| Ca44.12 | | | | | | | | | | |
| V_L | 6454 | 0.007 | 1128 | 6460 | -1.778 | 1584 | 5650 | -3.065 | 2300 | 2977 |
| V_L | 3507 | -0.185 | 1100 | 3357 | | | | | 1484 | 2823 |
| CaMg44.13/21 | | | | | | | | | | |
| V_L | 6669 | -0.095 | 983 | 6603 | -1.825 | 1290 | 6043 | -2.877 | 2235 | 3683 |
| Ca38.26 | | | | | | | | | | |
| V_L | 6649 | -0.175 | 935 | 6536 | -0.451 | 1626 | 6225 | -5.123 | 2550 | 2860 |
| V_L | 3695 | -0.337 | | | | | | | 1610 | 3264 |
| Ca36.16 | | | | | | | | | | |
| V_L | 6592 | -0.285 | 969 | 6400 | -1.206 | 1297 | 6004 | -2.797 | 2630 | 3348 |
| V_L | 3776 | -0.538 | | | | | | | 1275 | 3230 |
| Ca12.37 | | | | | | | | | | |
| V_L | 6484 | -0.214 | 1022 | 6327 | -0.882 | 1244 | 6131 | -3.336 | 1895 | 3936 |
| Ca00.49 | | | | | | | | | | |
| V_L | 7041 | -0.028 | 1092 | 7019 | -0.442 | 1661 | 6567 | -8.233 | 2200 | 3324 |

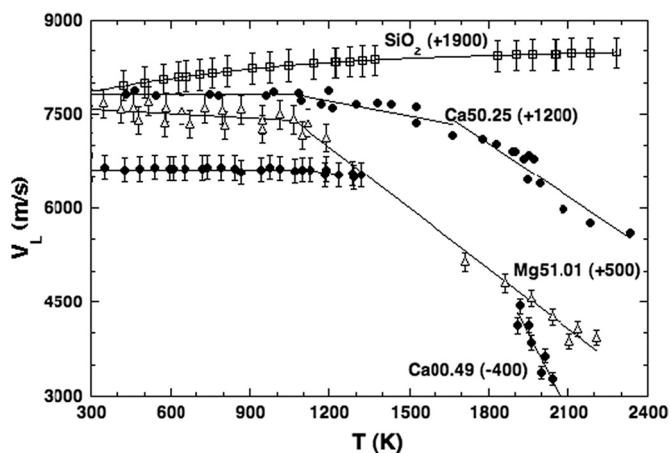


Fig. 7. Examples of difficulties met when measuring longitudinal wave velocities: data scatter for Ca50.25, and wide measurement gaps for Mg51.01 and Ca00.49. Measurements for SiO₂ included for comparison [8]. Data displaced vertically for the sake of clarity by the amounts indicated in parentheses. Linear-fit parameters reported in Table 5.

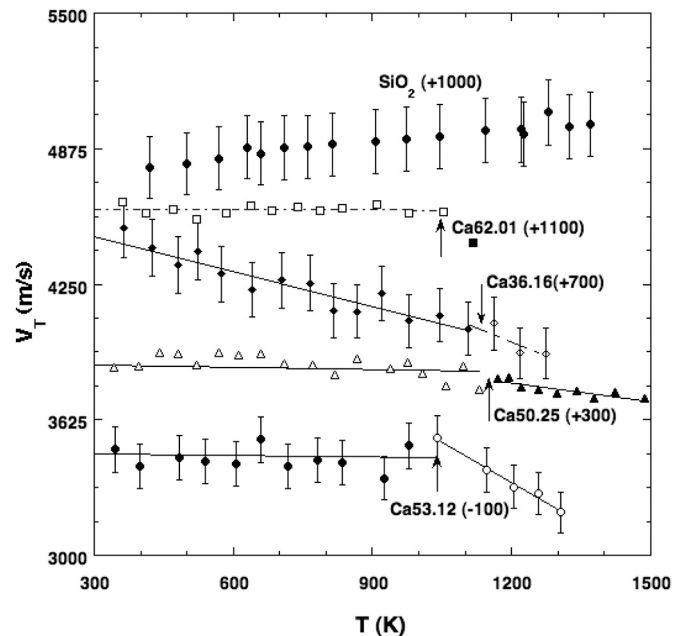
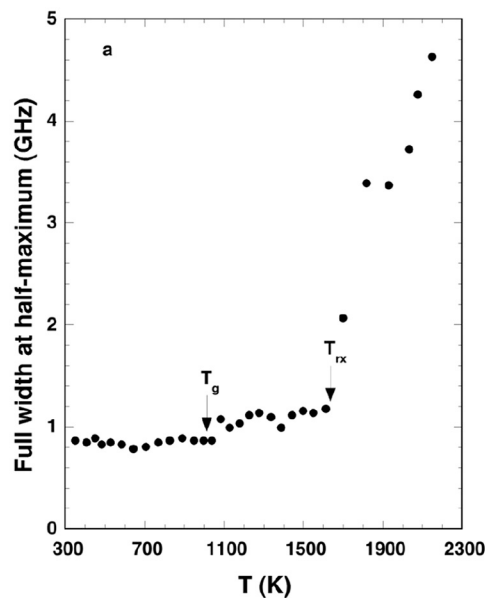


Fig. 8. Differing temperature dependences of the transverse wave velocities exhibited in some samples. Data for SiO₂ included for comparison [8]. Standard glass transition temperatures are indicated by the arrows. Data are shifted vertically for the sake of clarity by the amounts indicated in parentheses. Linear-fit parameters reported in Table 5.

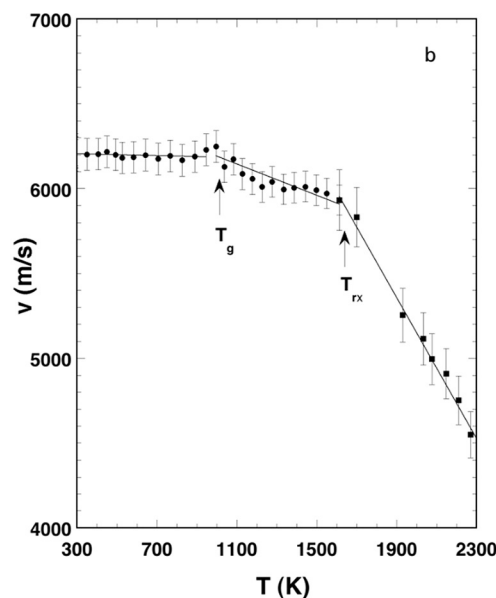


Fig. 9. (a) Variation of the Full Width at Half Maximum of the Brillouin peaks of Ca65.09 with increasing temperatures. (b) Determination of the temperatures T_g (1015 K) and T_{rx} (1641 K) of (a) from the positions of the breaks in the V_L plot. Linear-fit parameters reported in Table 5.

composition by about 35%. For aluminosilicate liquids, the average value of G_s at T_g is about 35 GPa, i.e., it is 3.5 times greater than the value of 10 GPa that is generally assumed for silicate liquids [27]. The exceptional variation of $G_s(\text{SiO}_2)$ was calculated from the V_T measurements [8].

In contrast to glasses, liquids cannot support permanent shear stress but propagation of shear waves has nonetheless long been known in the supercooled state [28]. Shear-wave propagation in liquids below T_{eq} is related to the presence of structured regions with dimensions large enough that, for a short time, shear stress can be stored as potential energy before being dissipated as a result of particle diffusion [29,30]. Molecular dynamics simulations on different liquids have shown that the size of systems needed for complete stress relaxation under strain

decreases with increasing temperature [30]. Hence it is via the temperature dependence of the size of structured units in the liquid that the propagation of transverse waves depends on frequency and becomes eventually impossible as a result of too fast structural relaxation.

Adam and Gibbs [31] postulated the existence of such structured regions and their diminishing size with increasing temperature to explain the observed changes in relaxation times with temperature in real liquids. The relevance of Adam-Gibbs theory to account for structural relaxation in silicate liquids has been discussed in relation to the fact that viscosity, enthalpy, and volume relaxation kinetics are almost the same in the glass transition range [32]. Given that our Brillouin observations were made at 50 K intervals, the T_g values listed in Table 5 are quite close to values determined for viscosity, enthalpy and volume relaxations [32,33]. The explanation for the damping of V_T in silicate liquids would in fact provide a way to evaluate the size and temperature

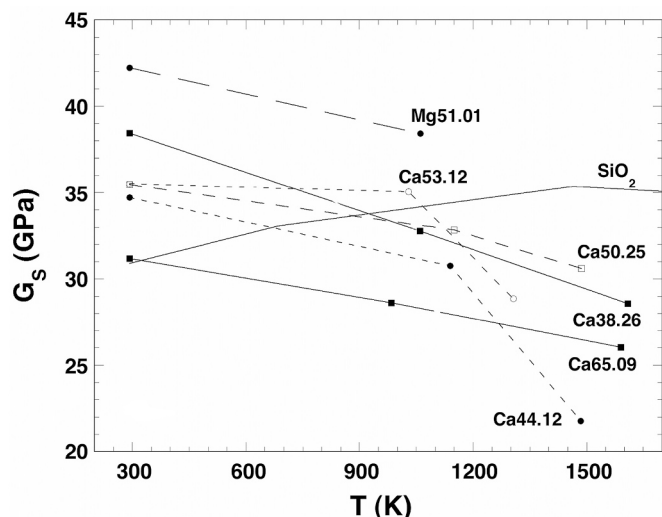


Fig. 10. Shear modulus at a frequency of about 10 GHz derived from the measured transverse velocities and ancillary density data (lines are guides for the eyes).

dependence of the Adam-Gibbs cooperatively rearranging regions from the infinite frequency shear stress modulus and the viscosity of the melt.

In all cases, the Brillouin peaks are rather narrow below T_g where they begin to broaden as a result of increasing topological disorder induced by increasing temperatures. Sound attenuation also becomes stronger above T_g . Although the theory of sound attenuation in glasses and liquids is not yet well established, thermal vibrations induce ultrasonic and hypersonic sound attenuation [34].

That broadening of Brillouin peaks reflects the increasing number of atomic configurations becoming accessible above the glass transition agrees with the near coincidence between T_g and the onset temperature of peak broadening (Fig. 9). The FWHM should be related to configurational entropy which also increases with rising temperatures above T_g . This hypothesis is supported by the fact that, like $\log(\text{FWHM})$, the configurational entropy of Ca50.25 and CaMg50.25/23, and silicate liquids in general, depends linearly on reciprocal temperature [33]. The inherent structure dynamics model for liquids also agrees with this implication [35,36]. At a microscopic level, however, the causes of changes in thermodynamic and kinetic properties of liquids above T_g are still being discussed.

4.3. Composition effects: compression mechanisms

Below 1400 K addition of CaAl_2O_4 to a melt or glass causes an increase of V_L . This trend is more or less shown by the data for the samples Ca50.25 and Ca00.49 with $R = \text{CaO}/\text{Al}_2\text{O}_3 \simeq 1$; for Ca38.26 and Ca12.37 with $R \simeq 1.4$; and for Ca65.09, Ca53.12 and Ca36.16 with $R \simeq 2.9$, (Fig. 11). The same trend is observed below 1400 K for compositions with approximately 50 mol% CaO, namely Ca50.00, Ca36.16, Ca12.37 and Ca00.49 whose V_L values increase with the CaAl_2O_4 content. At temperatures higher than 1400 K, however, replacement of CaAl_2O_4 by SiO_2 leads to higher V_L values. This is shown by SiO_2 whose V_L values are 5953 and 6555 m/s at 293 K and 2000 K [8], whereas they are 7044 and 3973 m/s respectively, for Ca00.49. In absence of Al_2O_3 , addition of CaO or MgO to SiO_2 causes an increase of V_L at low temperature (Fig. 11c), an effect that is stronger for MgO than for CaO (Fig. 11).

Evidently, the longitudinal sound velocity in silicate melts depends on melt structure, which is affected by temperature, chemical composition and pressure (which needs not to be considered here). The velocity of longitudinal waves is related to compressibility, see eq. (2) and (3), which depends on the overall rigidity of the internal structure of the melt or glass. Roughly speaking, the backbone of the internal structure is

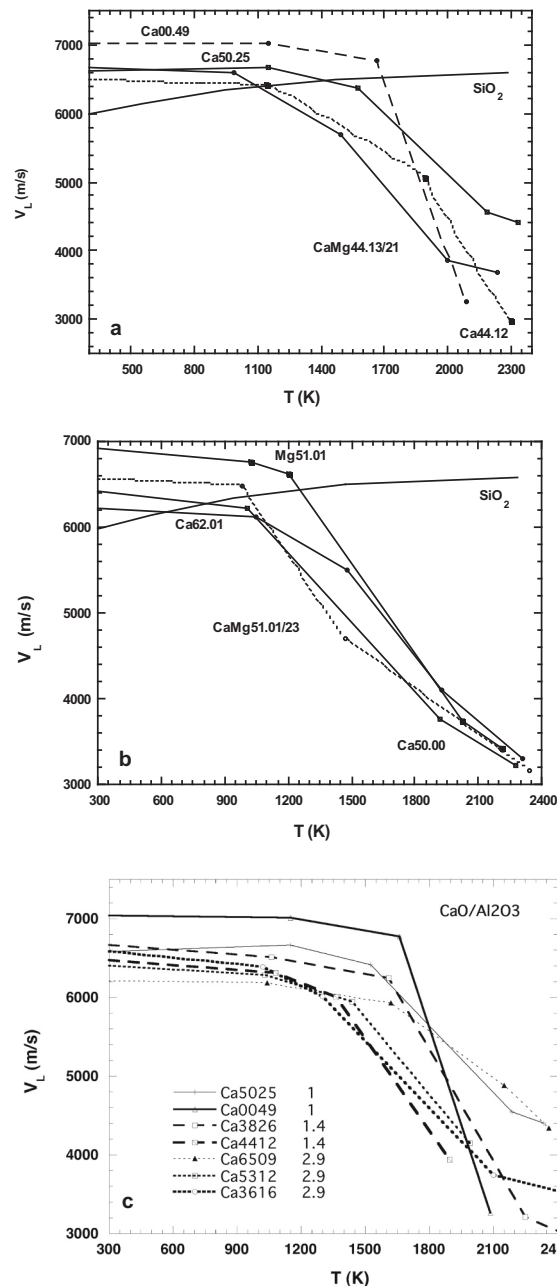


Fig. 11. Effects of composition of the longitudinal hypersonic sound velocity: (a) effect of CaAl_2O_4 or $(\text{Ca,Mg})\text{Al}_2\text{O}_4$ addition to SiO_2 ; (b) addition of CaO and/or MgO to SiO_2 ; (c) change of the molar $\text{CaO}/\text{Al}_2\text{O}_3$ ratio. (lines are guides for the eyes).

made up of corner-linked SiO_2 , $\text{Mg}_{0.5}\text{AlO}_2$ and $\text{Ca}_{0.5}\text{AlO}_2$ units. An excess of MgO or CaO with respect to what is needed to ensure charge compensation of Al^{3+} weakens the structure (Fig. 10). Temperature increases also weaken the internal structure, but the extend of this effect depends on composition and temperature. We thus conclude that addition of CaAl_2O_4 and MgAl_2O_4 strengthens the internal structure at low temperature, but weakens it at high temperature. This trend is well illustrated by $V_L(\text{SiO}_2)$, which is higher than that of any other silicate melt above 1700 K. Hypersonic velocity data indicate that MgAl_2O_4 is a stronger network former than CaAl_2O_4 at low temperature, but that the opposite holds true at high temperatures. These observations conform to what has been observed by geochemists and petrologists [37].

Declaration of Competing Interest

The authors declare that they have no known competing financial interests or personal relationships that could have appeared to influence the work reported in this paper.

Acknowledgments

P. Courtial is gratefully thanked for providing us with the samples used in this study. This work is of course dedicated to C.A. Angell whose ideas were so influential over the years. A touching aspect of his warm personality was revealed by a message sent to the first author ending with “à l’avenir” the day before he passed away. Sadly, Y. Bottinga followed him four months later (obituary in English and French at <https://www.ipgp.fr/fr/institut/hommage-a-yan-bottinga-1932-2021>).

References

- [1] J.A. Xu, M.H. Manghnani, *Phys. Rev. B* 46 (1992) 640–645.
- [2] J.A. Xu, M.H. Manghnani, P. Richet, *Phys. Rev. B* 46 (1992) 9213.
- [3] V. Askarpour, M.H. Manghnani, P. Richet, *J. Geophys. Res.* 98 (1993) 17683.
- [4] J. Kieffer, J.E. Masnik, B.J. Reardon, J.D. Bass, *J. Non-Cryst. Solids* 183 (1995) 51.
- [5] J.E. Masnik, J. Kieffer, J.D. Bass, *J. Chem. Phys.* 103 (1995) 9907.
- [6] D. Vo-Thanh, Y. Bottinga, A. Polian, P. Richet, *J. Non-Cryst. Solids* 351 (2005) 61.
- [7] D. Vo-Thanh, A. Polian, P. Richet, *Geophys. Res. Lett.* 23 (1996) 423.
- [8] A. Polian, D. Vo-Thanh, P. Richet, *Europhys. Lett.* 57 (2002) 375.
- [9] L.N. Sokolov, V.V. Baidov, L.L. Kunin, V.V. Dymov, *Sb. Tr. Tsentr. Nauch. Inst. Chern. Metall.* 75 (1971) 53.
- [10] S. Webb, P. Courtial, *Geochim. Cosmochim. Acta* 60 (1996) 75.
- [11] P. Courtial, D.B. Dingwell, *Amer. Min.* 84 (1999) 465.
- [12] P. Courtial, D.B. Dingwell, *Geochim. Cosmochim. Acta* 59 (1995) 3685.
- [13] P. Richet, P. Gillet, A. Pierre, M.A. Bouhifd, I. Daniel, G. Fiquet, *J. Appl. Phys.* 74 (1993) 5451.
- [14] J.R. Sandercock, In: *Light Scattering in Solids III, Topics in Applied Physics* vol. 51, Springer, Berlin, 1982, p. 173.
- [15] R.A. Lange, I.S.E. Carmichael, *Geochim. Cosmochim. Acta* 51 (1987) 2931.
- [16] R.A. Lange, *Contrib. Mineral. Petrol.* 130 (1997) 1.
- [17] J. Gottsmann, D.B. Dingwell, *Contrib. Mineral. Petrol.* 139 (2000) 127.
- [18] M.J. Toplis, P. Richet, *Contrib. Mineral. Petrol.* 139 (2000) 672.
- [19] R. Knoche, D.B. Dingwell, S.L. Webb, *Geochim. Cosmochim. Acta* 56 (1992) 689.
- [20] F.R. Schilling, S.V. Sinogeikin, M. Hauser, J.D. Bass, *J. Geophys. Res.* 108 (2001), <https://doi.org/10.1029/2001JB000517>.
- [21] A. Hushur, M.H. Manghnani, Q. Williams, D.B. Dingwell, *Am. Mineral.* 98 (2013) 367.
- [22] L.N. Sokolov, V.V. Baidov, L.L. Kunin, V.V. Dymov, *Sb. Tr., Tsentr. Nauch. Inst. Chern. Metall.* 75 (1971) 53.
- [23] M.L. Rivers, I.S.E. Carmichael, *J. Geophys. Res.* 92 (1987) 9247.
- [24] A.M. Nikonov, A.V. Bogdanov, D.V. Nemilov, A.A. Shono, V.N. Mikhailov, *Fyz. Khim. Stekla* 8 (1982) 694.
- [25] L. Comez, D. Fioretto, F. Scarfoni, *J. Chem. Phys.* 119 (2003) 6032.
- [26] J. Tauke, T.A. Litovitz, P.B. Macedo, *J. Amer. Ceram. Soc.* 51 (1968) 158.
- [27] D.B. Dingwell, S. Webb, *Eur. J. Mineral.* 2 (1990) 427.
- [28] G. Harrison, *The Dynamic Properties of Supercooled Liquids*, Academic Press, New York, 1976.
- [29] R.D. Mountain, *J. Chem. Phys.* 102 (1995) 5408.
- [30] J. Petravic, *J. Chem. Phys.* 120 (2004) 10188.
- [31] G. Adam, J.H. Gibbs, *J. Chem. Phys.* 43 (1965) 139.
- [32] A. Sipp, P. Richet, *J. Non-Cryst. Solids* 298 (2002) 202.
- [33] A. Sipp, Y. Bottinga, P. Richet, *J. Non-Cryst. Solids* 288 (2001) 166.
- [34] J. Fabian, P.B. Allen, *Phys. Rev. Lett.* 82 (1999) 1478.
- [35] F. Sciortino, W. Kob, P. Taraglia, *Phys. Rev. Lett.* 83 (1999) 3214.
- [36] S. Mossa, G. Monaco, G. Ruocco, M. Sampoli, F. Sette, *J. Chem. Phys.* 116 (2002) 1077.
- [37] B.O. Mysen, P. Richet, *Silicate Glasses and Melts*, Elsevier, Amsterdam, 2018.